HYDROLOGICAL PROCESSES
Hydrol. Process. (2010)
Published online in Wiley InterScience
(www.interscience.wiley.com) DOI: 10.1002/hyp.7630

Visualizing meltwater flow through snow at the centimetre-to-metre scale using a snow guillotine

Mark W. Williams,[1]* Tyler A. Erickson[2] and Jennifer L. Petrzelka[1]

[1] *Institute of Arctic and Alpine Research and Department of Geography, University of Colorado at Boulder, UCB 450, Boulder, CO 80309, USA*
[2] *Michigan Tech Research Institute and Department of Civil and Environmental Engineering, Michigan Technological University, 3600 Green Court, Suite 100, Ann Arbor, MI 48105, USA*

Abstract:

Movement of liquid water through snowpacks remains one of the least understood aspects of snow hydrology. Liquid water movement through snowpacks is generally recognized to occur in distinct flow paths rather than as uniform flow through a homogeneous porous medium. Dye tracer experiments have been used in studies of meltwater flow through snow since the 1930s. Although dye tracer experiments have provided valuable qualitative information about meltwater pathways, quantitative descriptions of their spacing and location are not commonly available because of the difficulty in precisely excavating and measuring pathways. Here we provide a new proof-of-concept instrument we term a 'snow guillotine' that provides more quantitative information from dye tracer experiments conducted on melting snowpacks. Photographs are taken of each cross-section over a 1-m distance. Application of image processing and geostatistical analysis allows collection of high-resolution (1 cm^3), three-dimensional data on meltwater flow through a snowpack.

The results show preferential flowpaths, with the majority of vertical flow occurring in the upper 20–55 cm of the snowpack, while fewer preferential flowpaths are apparent below 100 cm. The number of vertical flowpaths in the upper half of the snowpack averaged almost 100 per m^2, with the highest number of flowpaths reaching almost 300 per m^2. Layer interfaces were found to significantly increase the volume of dye, indicating dominance by lateral flow at these boundaries. At each stratigraphic interface, the number of individual clusters decreased and it was more likely for a dyed pixel to be part of a large cluster. Geostatistical analyses showed that there were large increases in correlation lengths and the connectivity function at stratigraphic layers in contrast to low values between layers. For example, the buried ice layer in Experiment A at 169–170 cm showed separation distances of 20 cm. In contrast, two rows above this layer the separation distance was only 2 cm. Implementation of the snow guillotine provides the ability to conduct geostatistical analyses on field measurements of meltwater flow while providing three-dimensional, quantitative data of unprecedented spatial resolution. Copyright © 2010 John Wiley & Sons, Ltd.

Additional Supporting information may be found in the online version of this article.

KEY WORDS snow; meltwater; flowpaths; dye tracer; image processing; geostatistics

Received 4 September 2009; Accepted 25 January 2010

INTRODUCTION

Movement of liquid water through snowpacks is one of the least understood aspects of snow hydrology (Richter-Menge *et al*., 1991). It has an important influence on the timing and magnitude of snowmelt hydrographs (Caine, 1992) and on biogeochemical and geomorphological processes (Caine, 1995; Williams *et al*., 2009). A better physically based understanding of water flow through snow will permit wider applications of operational snowpack models (Blöschl and Kirnbauer, 1991) and allow for better prediction of year-to-year variability within a site (Melloh, 1999). Similarly, research on glacial hydrology has shown that a poorly understood part of this system is the routing of water through supraglacial snowpacks (Arnold *et al*., 1998). Better understanding of water routing to the englacial hydraulic system will facilitate better understanding of the role of water in basal sliding of glaciers (Fountain and Walder, 1998).

Much remains to be learned about meltwater flow through snow (Williams *et al*., 1999a). Movement of liquid water through snowpacks is generally recognized to occur in distinct flow paths rather than as uniform flow through a homogeneous porous medium. Seligman (1936) found that snowpack permeability was enhanced when flow channels were present in the snowpack. Oda and Kudo (1941) described flow fingers and flow along layer interfaces. Preferential flowpaths, ice layers and ice columns have been observed in many other studies, in a wide range of different geographical settings (e.g. Wankiewicz, 1978; Higuchi and Tanaka, 1982; Marsh and Woo, 1984a,b; Kattelmann, 1985, 1989; McGurk and Marsh, 1995).

However, attempts to characterize the spatial distribution of preferential flowpaths have had only limited success (e.g. Marsh and Woo, 1985; Kattelmann, 1989).

* Correspondence to: Mark W. Williams, Institute of Arctic and Alpine Research and Department of Geography, University of Colorado at Boulder, UCB 450, Boulder, CO 80309, USA.
E-mail: markw@snobear.colorado.edu

Attempts to understand meltwater flow through snow from first principles have also had only limited success (e.g. Colbeck, 1979, 1991). An understanding of the spatial distribution of preferential flowpaths in melting snowpacks has suffered from the ephemeral nature of the flowpaths and the problems caused by destructive sampling of the snowpack (e.g. Schneebeli, 1995). There have been several attempts at modelling water flow through snow (Colbeck, 1975, 1979; Marsh and Woo, 1984b; Gustafsson *et al*., 2004). However, the lack of data on flowpath processes continues to limit progress in snowmelt modelling (Gustafsson *et al*., 2004). The ability to characterize the spatial distribution of these meltwater flowpaths would be useful in developing snowmelt runoff models which could better characterize snowmelt hydrographs (Waldner *et al*., 2004; Campbell *et al*., 2006).

Dye tracer experiments have been used in studies of meltwater flow through snow since Seligman's work in the 1930s (Seligman, 1936). In the US, dye was first used to trace flow paths in draining snowpacks during the Cooperative Snow Investigations (Gerdel, 1948, 1954; US Army, 1956). Through the application of a dye to the surface of a snowpack and subsequent snowpit excavation, dye tracers allow visualization of flow paths and formation of structurally different layers (Seligman, 1936; Schneebeli, 1995; Waldner *et al*., 2004; Campbell *et al*., 2006). Dye tracers coupled with flourometers measure dye concentrations over time so that liquid water contents and rates of movement can be calculated (Waldner *et al*., 2004; Campbell *et al*., 2006). Although dye tracer experiments have been able to identify the existence of meltwater pathways, quantitative descriptions of their spacing and location are not commonly available because of the difficulty in precisely excavating and measuring pathways.

Here we introduce a novel method of using dye tracers to provide quantitative statistics of meltwater flow through snow. Our 'snow guillotine' was inspired by the 'cutter box' of McGurk and Marsh (1995). They developed a method for quantifying the spatial distribution of flowpaths using a metal framework (36 cm $\times$ 36 cm) with an attached blade that sliced uniform thick-cut sections (2·5 cm or 3·8 cm) of a snowpack. Using light transmission, photographs were taken of the thick-cut sections to identify flow paths. The 'cutter box' allowed McGurk and Marsh (1995) to estimate finger size and spacing in a warm snowpack and to examine the vertical alignment of the fingers, both within storm layers and across inter-storm melt-freeze crusts.

The snow guillotine consists of a metal and PVC framework with an attached blade that slices uniform cross-sections (about 1 m $\times$ 1 m) at 1-cm intervals (or whatever interval the user desires) of a snowpit where dye tracer has been applied. Digital images are taken of each cross-section after the blade has removed a uniform section from the snowpack. Application of image processing techniques allows collection of high-resolution, three-dimensional (3D) data on dye presence that provides information on meltwater flow through a snowpack.

After the digital images are processed, geostatistical analyses are possible, such as correlation lengths (Erickson *et al*., 2005) and connectivity statistics (Western *et al*., 2001). Application of these quantitative techniques allows us to address questions such as: (1) What portion of the snowpack transmits meltwater? (2) Under what conditions do vertical meltwater pathways occur? (3) Are vertical meltwater flowpaths continuous across layer boundaries? (4) Can dye tracer experiments be used to identify snowpack layer transitions that cannot be easily identified from snowpit sampling? Furthermore, these datasets may allow for the future development and testing of two- and 3D physically based snowmelt models, as well as for the validation of non-destructive sampling techniques.

SITE DESCRIPTION

This study was conducted in 2003 in a forest clearing near tree line at the high-elevation (3360 m) Soddie site, within the Niwot Ridge, Colorado, Long-Term Ecological Research (NWT LTER) area (40·0480 °N, 105·5726 °W). This site has an underground laboratory $10' \times 30' \times 8'$ in size, line power and an array of snow lysimeters (Williams *et al*., 2009) (Figure 1). Adjacent to the underground laboratory is a suite of meteorological instruments sufficient to close the energy balance. Snowpits were sampled approximately weekly for physical and chemical parameters about 100 m from this experimental site (Figure 1) so as not to disturb the natural snowcover and lysimeters. The snow guillotine experiments were conducted adjacent to the snowpit location.

Snow cover at the site generally lasts from October to June. The SnoTel network operates the NIWOT 663 site at C-1 which is about 2 km from the Soddie site (Figure 1), providing long-term measurements of snow water equivalent. The continental, high mountain climate of Niwot Ridge has been recorded continuously at the D-1 meteorological station on Niwot Ridge since the early 1950s. Located about 5 km from the Soddie site at an elevation of 3750 m, D-1 mean annual temperature is $-3{\cdot}7\,^{\circ}\mathrm{C}$ (Williams *et al*., 1996), with night-time temperatures during the winter often falling below $-30\,^{\circ}\mathrm{C}$. Almost 80% of the approximately 1000 mm of annual precipitation falls as snow (Caine, 1996).

METHODS

Dye tracer

We conducted two experiments where a dye tracer was applied to the surface of a wet and draining snowpack in an attempt to visualize flowpaths within the snowpack. Dye tracers have frequently been used to characterize water flow and solute transport in soils (e.g. Flury and Wai, 2003). We used the food dye Brillant Blue FCF,

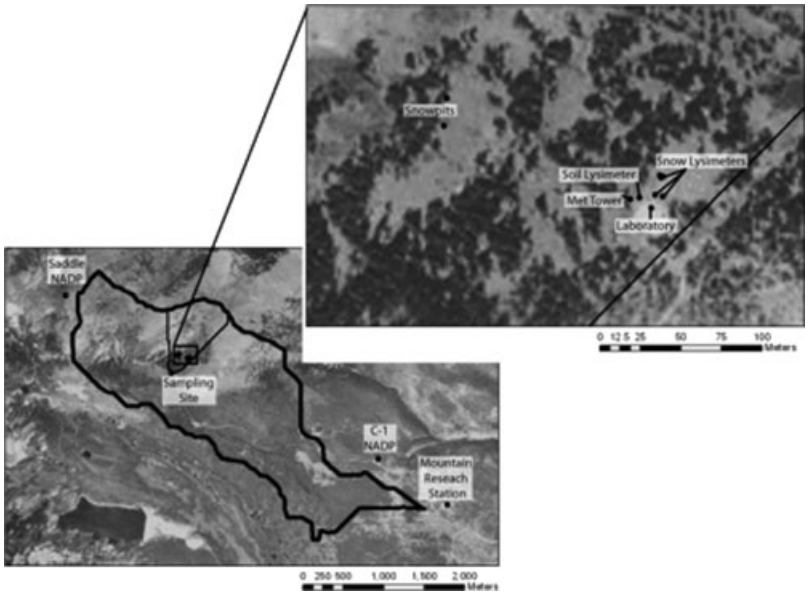

Figure 1. Location and site map of the experimental area on Niwot Ridge, Colorado. The Soddie site is the expanded area, with sampling sites shown for the snowpits (and snow guillotine experiments), the meteorological station, snowmelt lysimeters and the Soddie underground laboratory. Delineations indicate the Como Creek watershed and the headwater basin boundaries. The SnoTel site is located at C-1. Adapted from Williams *et al*. (2009)

which has been used to investigate infiltrating snowpack meltwater into high-elevation soils (Stähli *et al*., 2004). The dye has relatively low toxicity to organisms and is therefore suitable for use in environmental studies (Flury and Flühler, 1995). Brilliant Blue FCF readily dissolves in water, and is highly visible in snow. Flury and Flühler (1995) demonstrated that in a loamy sand this tracer was only slightly retarded in infiltrating water (relative retardation 1·2) compared to the conservative tracer Iodit.

Snow properties

Snowpits were sampled about every two weeks at the Soddie site following the protocols of Williams *et al*. (1999b). Density was measured in vertical increments of 10 cm using a Snowmetrics 1-l (1000 cm^3) stainless-steel cutter and an electronic scale (±2 g). Temperature of the snowpack was measured every 10 cm with 20-cm-long dial stem thermometers, calibrated using a one-point calibration at 0 °C. The height of stratigraphic layers above the snow/ground interface was recorded, along with the thickness and type of layer (melt/freeze crust, ice layer, rounded grains), and grain type and grain size of each layer were determined using a 10× magnifying loupe and a gridded crystal card, and described following the protocols in The International Classification for Seasonal Snow on the Ground (Colbeck *et al*., 1990). Prior to each guillotine experiment, a snowpit was excavated to sample snow properties from the snow/air interface to the snow/ground interface using the same protocols. The working wall of the snowpit was oriented so that it remained shaded from the sunlight and unaffected by the applied dye throughout the sampling period. For each experiment, the working wall of the pit was approximately 1 m from the location of the guillotine.

Snowpack meltwater production

Release of meltwater from the snowpack was investigated by collecting snowpack meltwater in 0·2-m^2 snow lysimeters before contact with the ground following the protocol of Williams *et al*. (2009). Meltwater flowed by gravity from the snow lysimeters into the subnivian laboratory. Meltwater discharge for each snow lysimeter was measured continuously in individual tipping buckets at 10-min intervals (hand calibration showed that one tip was equal to 11 ml). A total of 106 snowpack lysimeters were deployed in 2003.

Snow guillotine

The guillotine instrument is a rigid frame designed to guide a blade that cuts a thin plane of snow from the working wall of a snowpit (Figure 2). The PVC frame rests on the snow surface and is attached to the snowpack with snow anchors and cam straps (Figure 2). An upright metal support holds the metal cutting frame perpendicular to the snow surface and is advanced along the PVC frame. A stainless-steel cutting blade is attached to the bottom of the cutting frame, similar to the 'cutting box' of McGurk and Marsh (1995). The blade moves downward and parallel to the sidewall of the snowpit shaving a thin layer of snow with each downward pass. The thickness of the section that is planed off the wall of the snowpit is determined by the user. The entire guillotine weighed approximately 25 kg and disassembled to fit into a large ski bag.

A Nikon Coolpix 995 3-MegaPixel digital camera was used to record images of the shaved face of the snowpit. The camera was suspended a fixed distance away from the snowpit face by means of an aluminium frame (Figure 2). A digital image was taken after each pass of the cutting blade when a new layer of the

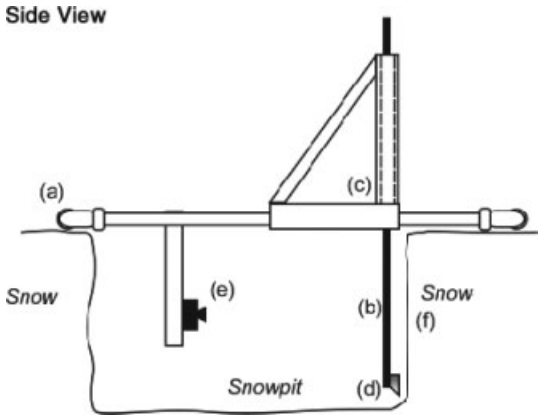

Figure 2. The snow guillotine consists of (a) a stationary PVC frame that rests on the snow surface, (b) a rectangular aluminium cutting frame that moves vertically and (c) a triangular frame that holds the cutting frame perpendicular to the stationary frame. A stainless-steel cutting blade (d) is attached to the bottom of the cutting frame. A digital camera (e) suspended below the PVC frame is used to obtain images of the shaved wall (f) of the snowpit

snowpack was exposed and when the cutting blade was in its lowest position. The vertical sides of the cutting frame were marked and visible in each image, so variations in the camera orientation can be corrected. Fourteen horizontal markers were placed on the vertical members of the cutting frame to use as control points for georectification of each image. For each of the two experiments photographs were taken every 1 cm over a distance of 100 cm. The dimensions of the cutting frame were 0·94 m in width and 1·19 m in height. The steps required to obtain a single image were as follows:

1. The cutting blade was raised to its highest position.
2. The frame was advanced horizontally a distance of 1 cm.
3. The cutting blade was lowered, shaving a uniform plane 1 cm in thickness from the imaging face of the snowpit.
4. An image of the exposed face was recorded with the digital camera.
5. The frame was advanced horizontally a distance of 1 cm and the procedure repeated until a sufficient volume of the snowpack had been sampled (typically 100 images).

Each experiment thus produced 100 images taken every 1 cm, with the dimensions of each image about 100 cm $\times$ 100 cm.

Image processing

A series of steps were used to process the individual images captured by the digital camera. The digital images were georectified and resampled using ENVI image processing software. The image was resampled to pixels 1 cm^2 in area, to match the thickness of each cut. The images from each experiment were then merged to create a 3D cube of relative dye concentrations. Each 3D pixel (or voxel) represents the relative dye concentration in a 1-cm^3 volume.

To account for the variable illumination encountered throughout the experiment, a colour band ratio image of the snowpit wall was constructed. The original colour image consists of red, green and blue bands, each with different sensitivities to the dye, but similar responses to variable illumination. By dividing one colour band in which the dye is highly visible by that of a band where the colour is not visible, a high-contrast image is produced that is a function of dye concentration. Since we applied a Brillant Blue tracer to the melting snowpack, we used the red : blue ratio.

Throughout the snowpack, the dye concentration changes as dyed surface meltwater mixes with that of undyed liquid water in the snowpack. As a result of this mixing, the band ratio value is a continuous variable. Thus, there will be continuous dye concentration values, making it difficult to separate dyed voxels from undyed voxels as the dye concentration becomes low. In the remote sensing community, commonly used techniques such as single band ratios and the normalized difference snow index (NDSI) (Hall *et al*., 1995) take advantage of the high brightness values of snow and ice in the visible wavelengths to separate them from darker areas such as rock, soil or vegetation, using a threshold value to obtain a binary map of snow or glacier areas (Racoviteanu *et al*., 2008). To conceptually simplify our data set, a threshold value was chosen to separate meltwater with dye from background regions with no dye. The threshold value was selected based on visual comparison of an original image and a series of binary images based on different threshold values (Figure 6·5, Erickson, 2004), similar to the process used to separate glacier ice from non-glacial areas using ASTER imagery in the Cordillera Blanca of Peru (Racoviteanu *et al*., 2008). After choosing and applying a threshold value to the images, a data cube of binary values was formed in which each voxel (a 3D pixel) represents either a dyed voxel (dyed meltwater) or undyed voxel (no dyed meltwater).

The original coordinate system of the data cube was oriented with the plane of the snow surface because the cutting blade was positioned perpendicular to the snow surface (Figure 2). However, due to differential settling and ablation rates, the snowpack layer interfaces were not always parallel to the snow surface. In order to analyse changes across snow layer interfaces we altered the coordinate system so that the axes were aligned to the snowpack stratigraphy, not the snow surface. A new coordinate system that was parallel to the layer interfaces was established. Voxel values were determined using nearest neighbour interpolation with the new coordinate system. The edges of the newly interpolated data cube were then trimmed so that the edges were uniform.

Statistical analysis

Once the image was processed, certain parameters were defined in order to make statistical inferences. This was accomplished using what we term 'row statistics'. The horizontal plane of voxels corresponding to a particular row were analysed to develop a series of statistics for

the thresholded data cube. Each row consists of 10 000 voxels in a 1 m × 1 m × 1 cm matrix. Numbering of each row starts at the top of the image and the row number increases downwards towards the bottom of the snowpack. Each row was analysed to develop a series of statistics for each data cube. Row statistics are defined as follows:

Fraction dyed. The fraction of voxels in a row with dye, defined as the number of voxels below the threshold binary value (low values have dye) divided by the total number of voxels in the row.

Clusters. The number of distinct clusters in a row. A cluster was defined as a set of interconnected voxels in which each voxel has eight neighbouring voxels it can be potentially connected to. Cluster sizes may range from a single voxel to an entire row of voxels.

Cluster size. The probability distribution function of the areal cluster size which represents the probability that an individual voxel is in a cluster of a given size. Cluster sizes may range from a single voxel to the entire row of voxels.

Vertical flowpaths. Describes the transition probability of individual voxels between adjacent rows (moving from the snow surface to the base of the snowpack). Three transition probabilities were considered:

1. The individual voxel changed from dyed in the row above to non-dyed in the current row.
2. The voxel value remained the same in the row above and the current row.
3. The voxel value changed from non-dyed in the row above to dyed in the current row.

This group of statistics gives an indication of the continuity of distinct meltwater pathways between rows.

Correlation function. The spatial variation of the voxels within a row is characterized with an isotropic covariance function:

$$R(h) = E[(z(\boldsymbol{x}) - m(\boldsymbol{x}))(z(\boldsymbol{x}') - m(\boldsymbol{x}'))] \qquad (1)$$

where h is the scalar spatial separation distance between points $\boldsymbol{x}$ and $\boldsymbol{x}'$, z is the presence or absence of dye in a voxel, m is the trend of the variable, $R(h)$ is the covariance for points separated by distance h, and E [] denotes the expected value. We chose to model the spatial covariance function with an exponential model following the rationale in Erickson *et al*. (2005). Since we are primarily interested in the distance over which voxel values are correlated, the correlation function, $\rho(h)$, was defined by normalizing the covariance function ($R(h)$) by the variance ($R(0)$):

$$\rho(h) = \frac{R(h)}{R(0)} \qquad (2)$$

The correlation function of the binary voxels was calculated using bin separation intervals of integers between 0 and 25 cm. This statistic examines the lateral continuity of flow, with increasing correlation lengths (h) indicating increasing lateral continuity of flow.

Connectivity function. Describes the probability that two voxels separated by a given distance are part of the same cluster. Connectivity statistics have been shown to provide information about hydrologically connected variables that cannot be obtained by relying solely on indicator statistics of correlation functions, which only describe the continuity of a variable (Western *et al*., 2001). We adopt the definition used by Western *et al*. (2001) to analyse soil moisture patterns, which defines the connectivity function $\tau(h)$ as the probability that a voxel in a cluster is connected to the set of voxels that are separated by the distance h:

$$\tau(h) = P(\boldsymbol{x} \leftrightarrow \boldsymbol{x}' | \boldsymbol{x} \in A, \boldsymbol{x}' \in G) \qquad (3)$$

where h = the distance of separation; G = the set of all voxels; A = the set of voxels with dye; $\boldsymbol{x}$ = a vector of coordinates of a voxel in A; $\boldsymbol{x}'$ = a vector of coordinates of a voxel in G; $h = ||\boldsymbol{x} - \boldsymbol{x}'||$, the separation distance; $\leftrightarrow$ denotes that two voxels are connected.

In practice, the separation distances, h, are binned into a series of separation ranges. Similar to the experimental correlation function, integer bin separation intervals between 0 and 25 cm were used.

RESULTS

The total winter accumulation of snow water equivalent at the nearby Niwot Ridge SnoTel site in 2003 was near the 20-year average. Maximum snow depth of 280 cm occurred during the first week of May, with a volume-weighted mean density of 392 kg m^{-3} and mean snow temperature of −0·27 °C. The snowpack became isothermal the second week in May, with the first meltwater recorded in snowmelt lysimeters on 16 May 2003. Numerous ice columns were found in snowpits from May but not in June.

The first snow guillotine experiment (Experiment A) was conducted on 23 May 2003 (Figure 3). Snow depth was 220 cm, with a depth-integrated density of 480 kg m^{-3}. The snowpack was isothermal at 0 °C throughout the experiment. Twelve layer interfaces were identified, most of which were buried melt/freeze and wind crusts. The ice/crust layers ranged from 0·5 to 3·0 cm in thickness. The upper 170 cm of the snowpack consisted of clustered rounded grains that had undergone significant wet metamorphism. The grains were in polycrystalline clusters about 2 mm in diameter. The lower 60 cm of the snowpack consisted of mixed forms of faceted crystals about 3 mm in diameter, with highly rounded corners. Snow melt lysimeters collected an average value of 36 mm of meltwater on 23 May 2003 (n = 34).

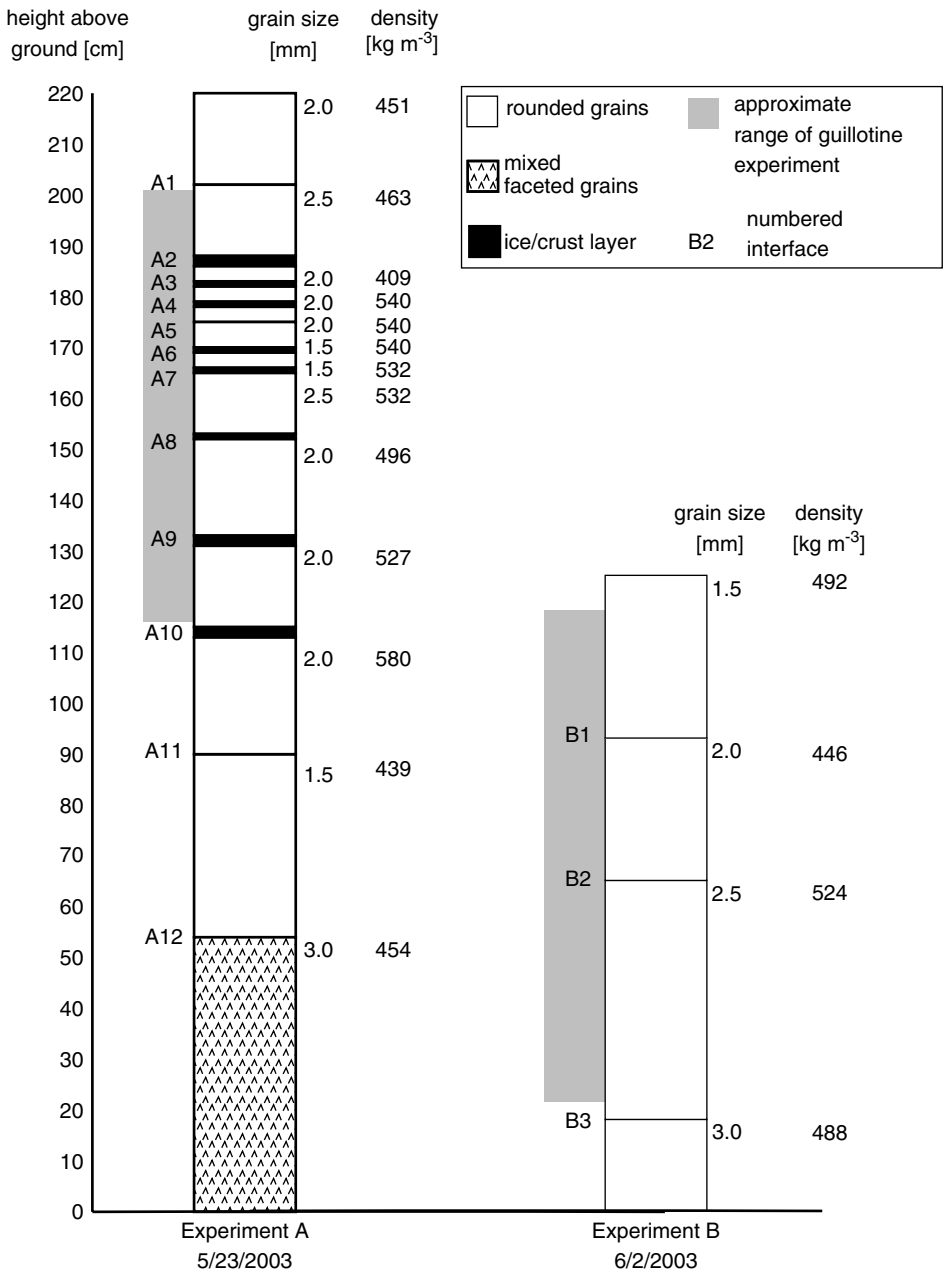

Figure 3. Snowpack stratigraphy from snowpits adjacent to snow guillotine experiments. Grey areas indicate the depths sampled by snow guillotine experiments. For all three snowpits, the temperatures throughout the snowpack were isothermal at 0 °C

During the 10 days between Experiment A and Experiment B on 2 June 2003, the snowpack ablated from 220 to 125 cm (Figure 3). Only three layer interfaces (B1–B3) were identified in the snowpit of Experiment B. These layers were thinner with less distinct layer interfaces than those of Experiment A. The faceted grains near the bottom of the snowpack in Experiment A were no longer present in Experiment B. While the apparent grain size remained similar between the two experiments, the effective grain size increased due to differences in grain morphology. Depth hoar has a long extension, but hollow features, whereas clustered rounded grains characteristic of melt are spherical in shape. The amount of snowmelt for Experiment B was similar to Experiment A at 34·4 mm d^{-1} ($n = 30$). Daily minimum air temperatures were at or above 0 °C from 23 May to 2 June. Thus, the stratigraphy for Experiment B was most likely the remnants from Experiment A.

Tracer application

Each snow guillotine experiment was started by spraying dye on the surface of the snowpack. Brilliant Blue FCF tracer was applied to the surface of the snowpack approximately 1–2 h prior to execution of the snow guillotine experiment to allow infiltration of the dye into the snowpack. The dye covered an area of approximately 3×3 m and was centred upslope of the guillotine cutting area. The dye was allowed to infiltrate into the snowpack, and additional dye was applied to the surface when the previous application faded. Approximately 8 l of water

with Brillant Blue dye were applied in both experiments over the timespan of an hour, an application rate of about 1 mm h^{-1} of liquid water over the dyed area. While the dye was infiltrating, an initial snowpit was excavated to monitor dye movement. After infiltration of the dye was complete, the guillotine experiment progressed by slicing 1-cm-wide cross-sections from the snowpit wall. The width of the snowpit was constrained by the PVC frame, while the minimum length of the snowpit was controlled by the viewing angle of the digital camera. The guillotine instrument and snowpack conditions after completion of Experiment A are illustrated in Figure 4. Dye accumulation along stratigraphic layers is clearly visible, as are preferential flowpaths between stratigraphic layers.

Image processing

Construction of data cubes from images collected during the snow guillotine experiments is illustrated for Experiment A in Figure 5. A colour image of an uncorrected image is shown in Figure 5a. Distortion by the camera lens is evident. Each digital image was georectified and resampled using ENVI image processing software with an area 100 cm × 100 cm (Figure 5b). A high-contrast image was then produced that distinguished dyed from undyed background voxels using a threshold value of 0·6 for the red : blue band ratio (Figure 5c), following the explanation in Erickson (2004). The complete series of individual images from Experiment A were then assembled into a data cube. The data cube was then rotated so that the axes of the data cube were parallel to the stratigraphic layers (2° in Experiment A) and cropped to remove the pixels at the top and sides of the snowpack (Figure 5d).

Figure 4. The guillotine instrument after completion of Experiment A (5/23/2003). Dye accumulation along stratigraphic layers is clearly visible in the imaged wall and the sidewall, along with vertical flowpaths between the stratigraphic layers. Note ski boot for scale

The basic elements or pixels in each data cube were voxels 1 cm^3 in volume and for which we know their *xyz* coordinates. The data cube can then be analysed in any number of configurations. One way to visualize the data cube is to make horizontal or vertical slices through the cube. Figure 6 shows a progression of horizontal row slices above and below the buried ice layer (layer A6) at 169–170 cm above the ground in Experiment A. Here we show the data cube after it has been georeferenced but before we have conducted the threshold filtering into dyed and undyed voxels, illustrating the full range of band ratios. Five different layers each 5 cm apart in depth (two sections above the buried ice layer, the ice layer, and two sections below) allows us to visualize changes in meltwater flowpaths with depth. Figure 6a and b exhibits a similar distribution of meltwater flowpaths with about 10% of each row containing dyed voxels, and the continuity of most flowpaths is clear between these two rows of the data cube. The percent coverage of dyed voxels increases to almost 60% at the ice layer (Figure 6c). Moreover, the intensity of dye increases at the ice layer, suggesting that the liquid water content is higher at the ice layer compared to the vertical flowpaths above. The meltwater flowpaths below the ice layer (Figure 6d and e) do not correspond to the meltwater flowpaths above the interface (6b), but are similar to each other.

Another method of evaluating the information in each data cube is to present an animation of each slice through the data cube. An animation based on the imagery illustrated in Figure 6 is available in supporting information.

Row statistics

For both experiments we performed statistical calculations on each row. These 'row statistics' were performed after the binary threshold function which separated the voxels into dyed and undyed voxels. The fraction of volume dyed increased between the two experiments and at layer interfaces within individual experiments. Experiment A had dyed fractions between 0·4 and 0·6 at or near layer interfaces, and fractions between 0·1 and 0·25 within layers (Figure 7a). The number of dyed voxels at all layer interfaces increased relative to the number of dyed voxels in rows above the layer interfaces. Layer interfaces identified by the tracer experiments were the same as that identified using normal snowpit protocols, with the exception of A5 (Figure 7a), a relatively subtle boundary between two rounded grain layers. For Experiment B, the average fraction of dyed area increased for both stratigraphic interfaces and the snowpack volume between interfaces in the upper portion of the snowpack. For example, almost 100% of the voxels had dye at the B1 layer at row 42, and the dyed fraction was generally greater than 60% between rows 42 and 51 (Figure 8a).

The number and size of clusters provides information on vertical and horizontal flowpaths. Small clusters are

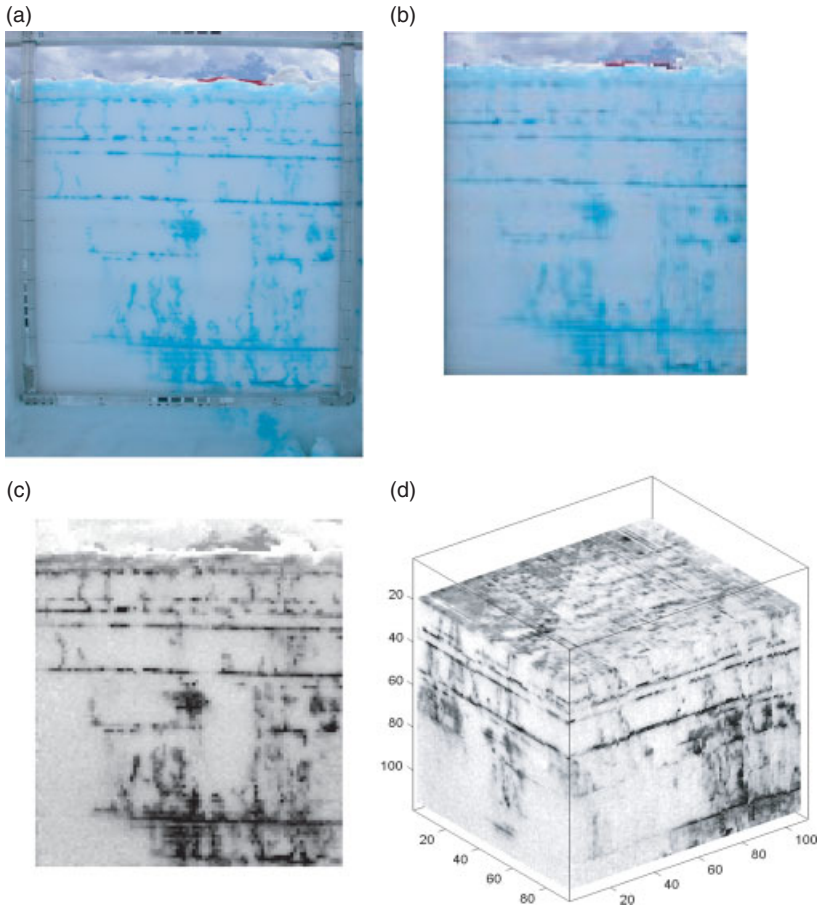

Figure 5. Data cube construction. A colour image (a) created by the digital camera is georectified using 14 reference marks located on the vertical sections of the cutting frame and resampled to 1-cm^3 pixels (b). A ratio image (c) is created using two of the RGB colour channels. The effect of variable illumination is reduced in the ratio image. Finally, the complete series of ratio images is assembled into a data cube (d). The dark areas represent high-volume dye concentrations (i.e. flowpaths) and the light areas represent low-volume dye concentrations, i.e. background flow. The datacube is rotated so that the axes are parallel to the stratigraphic layers and cropped to remove the pixels of the disturbed snow at the top and sides of the snowpack

indicative of vertical flow, while large clusters indicate lateral flow. If we assume that each cluster represents a vertical flowpath, in Experiment A the number of vertical flowpaths in the upper half of the snowpack averaged almost 100 per m^2, with the highest number of flowpaths reaching almost 300 at row 50 (Figure 7b). In contrast, in Experiment B the number of vertical flowpaths were generally less than 20 per m^2, except in the top 20 cm (Figure 8b). At each stratigraphic interface, the number of individual clusters decreased (Figures 7b and 8b) and it was more likely for a dyed voxel to be part of a large cluster (Figure 7c and 8c). Large clusters were associated with larger areas of dyed voxels compared to small clusters, which were associated with areas of less dyed voxels. For Experiment A, rows 20–55 were typically characterized by relatively high probabilities of small clusters between the layer interfaces (Figure 7c), while deeper in the snowpack (rows 55–100), the small clusters were not as common. In the deepest section of the snowpack (rows 100–114), small clusters were not apparent at all. Overall, these results suggest that vertical flowpaths were less distinct in Experiment B than in Experiment A, and in both experiments preferential flow was most prevalent in the upper layers of the snowpack.

Moving downward through the snowpack from the snow surface towards the ground, continuity (i.e. transitions) between layers was characterized by an increase or decrease in dyed voxels (Figures 7d and 8d). Within a section of the snowpack between stratigraphic boundaries such as ice layer, most of the voxels did not transition from dyed to non-dyed (or non-dyed to dyed), indicating that the location of the dyed areas were vertically continuous, e.g. vertical flowpaths.

The correlation function (Figures 7e and 8e) and the connectivity function (Figures 7f and 8f) provide an indication of the lateral continuity of the meltwater flowpaths. Both functions range between zero (no correlation/connectivity) and one (perfect correlation/connectivity), and summarize the variability as a function of horizontal separation distance. However, the connectivity function only considers pixels that are interconnected within the horizontal layers, whereas the correlation function does not differentiate between discontinuous and interconnected dyed voxels within a horizontal layer. Therefore, the connectivity function identifies layer interfaces more clearly than the correlation function due to the lateral flow of water at layer boundaries.

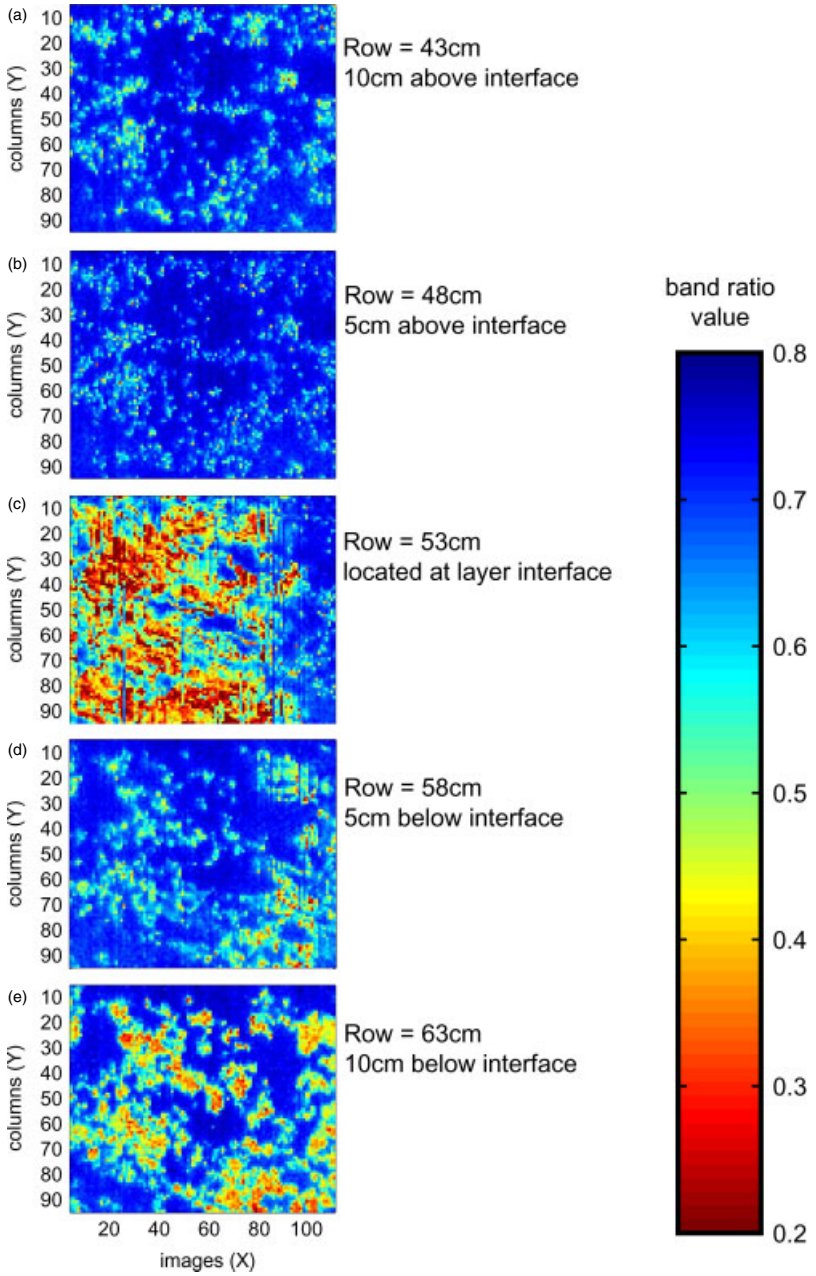

Figure 6. An example of horizontal slices from Experiment A. Each subfigure displays a row of the data cube, which is parallel to the snowpack stratigraphy. Subfigures (a) and (b) are above the ice layer interface, subfigure (c) is at the ice layer, and subfigures (d) and (e) are below the layer interface. Blue colour denotes low concentration dyed areas, while red colour denotes high concentration dyed areas

There were large increases in the connectivity function at stratigraphic layers in contrast to low values between layers (Figures 7f and 8f). For example, the buried ice layer in Experiment A (layer A6) at 169–170 cm showed separation distances of 20 cm. In contrast, two rows above this layer, the separation distance was only 2 cm. In general, there was little continuity in the separation distance for rows between stratigraphic layers. The connectivity function (Figures 7f and 8f) provides an indication of the vertical continuity of distinct meltwater flowpaths by illustrating relatively dramatic changes at interfaces and low horizontal connectivity within layers in the upper section of the sampled snowpack. Interestingly, the connectivity function was the only row statistic that differentiated between the rows above and below interface A5. Both the correlation function and connectivity function indicate that vertical flowpaths (suggested by low separation distances) were most continuous in the upper layers (e.g. Experiment A rows 22–28 and 40–52).

Comparison of Experiment A to Experiment B showed that many of the stratigraphic layers identified in Experiment A had disappeared over the 10-day period between the two experiments. The remaining layers were thinner with less distinct layer interfaces. Due to metamorphic processes, it is expected that the snow grains would be larger in the latter experiment, although snowpit sampling (Figure 3) indicated similar grain sizes for the two experiments. Similar to Experiment A, Experiment B illustrated

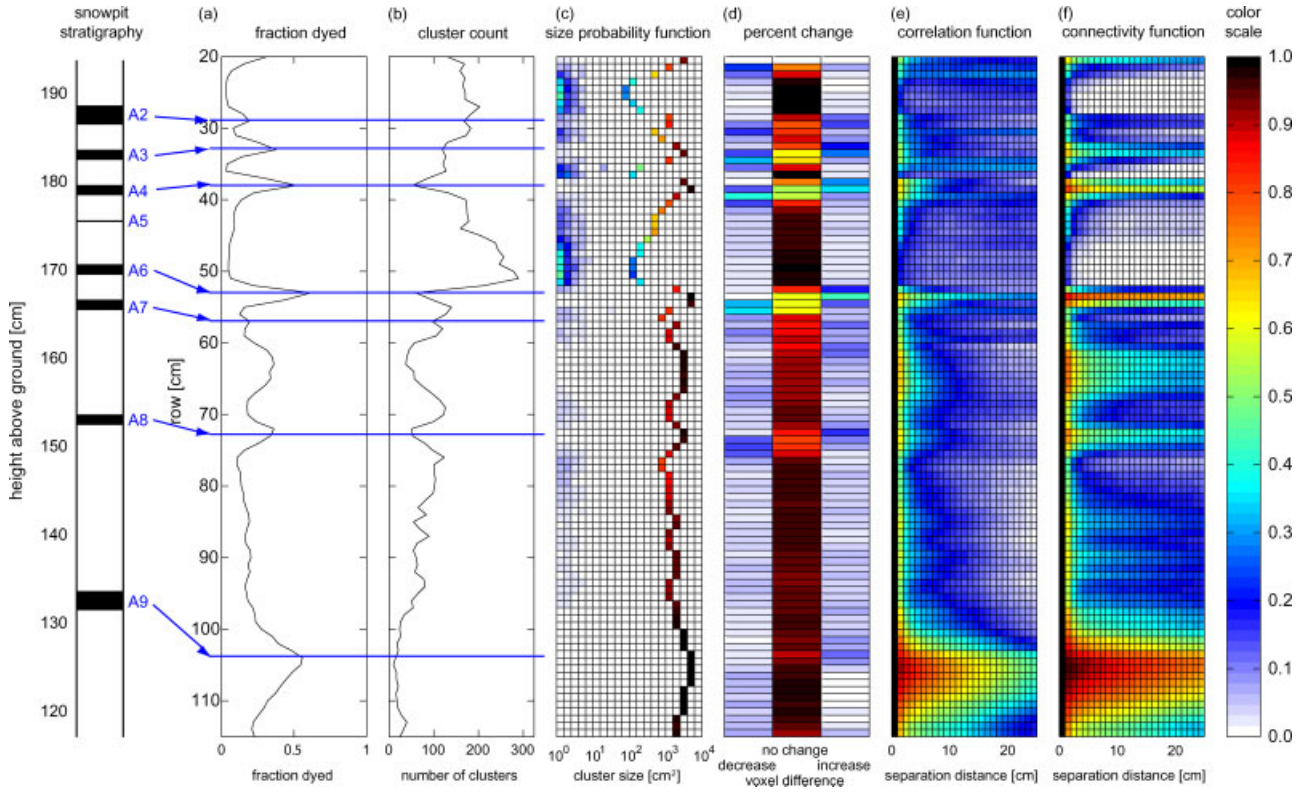

Figure 7. Experiment A row statistics (23 May 2003). For each row of voxels the (a) fraction dyed, (b) number of dyed clusters (interconnected group) per row, (c) cluster size probability function, (d) percent change plot, (e) correlation function and (f) connectivity function are presented. Colour scale ranges from 0 (white) representing no correlation/connectivity, to 1 (black) representing perfect correlation/connectivity

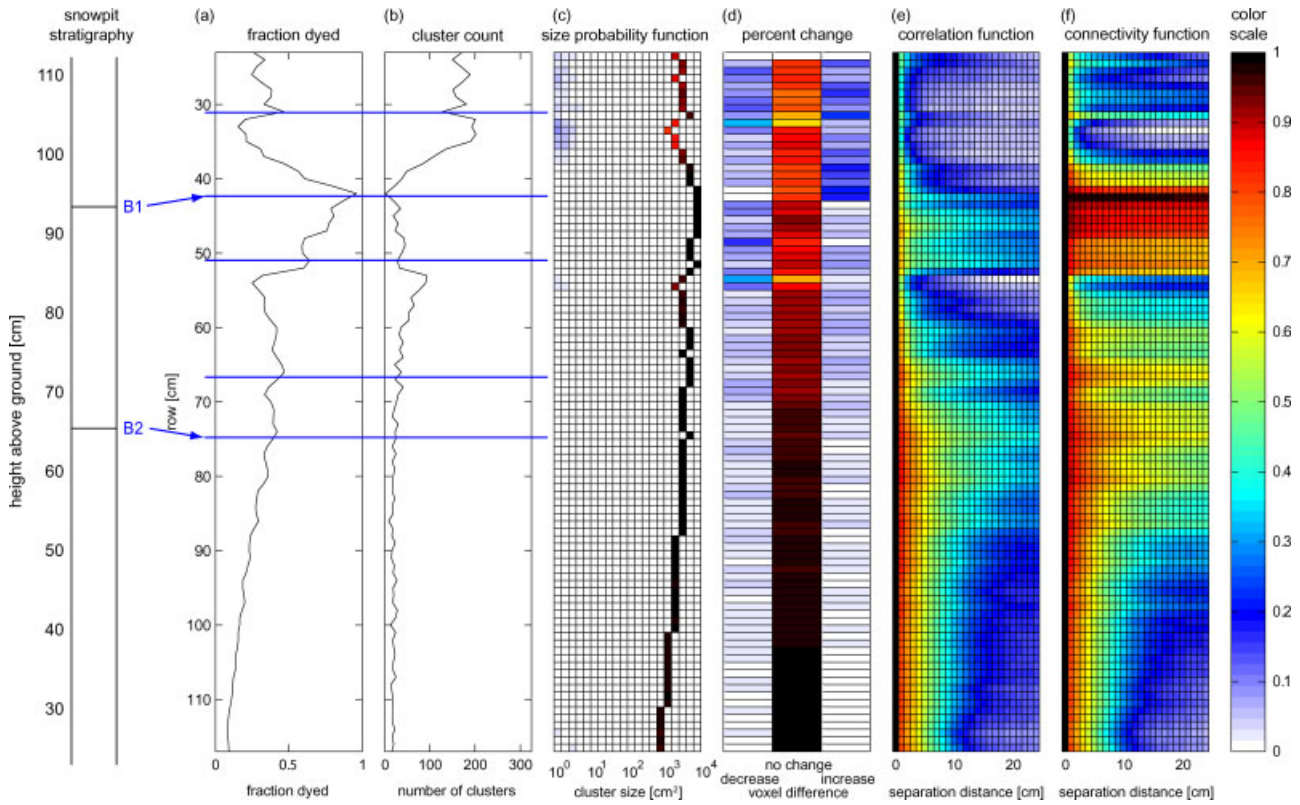

Figure 8. Experiment B row statistics (2 June 2003). For each row of voxels the (a) fraction dyed, (b) number of dyed clusters (interconnected group) per row, (c) cluster size probability function, (d) percent change plot, (e) correlation function and (f) connectivity function are presented. Colour scale ranges from 0 (white) representing no correlation/connectivity, to 1 (black) representing perfect correlation/connectivity

greater variability between rows in the upper part of the sampled snowpack (Figure 8c, d, f). Distinct flowpaths were found in the upper layers (Figure 8c; rows 23–37) but not in the lower layers. It is interesting to note that the existence of flowpaths identified in the upper layers of Experiment B were not apparent in Experiment A, even though the same layer was sampled (Figure 7; Experiment A; height 140–120). It is likely that flowpaths found in the upper layers of Experiment B formed in the time period between the experiments.

DISCUSSION

Each of the generated data cubes from this study exhibited evidence of preferential flowpaths. Experiment A had the most distinct meltwater flowpaths, with a decrease in the number of vertical flowpaths in Experiment B. This decrease is likely due to the amount of time the snowpack had been isothermal prior to sampling, and the extent of metamorphism that had taken place as a result. As explained by Colbeck (1979), as snowpacks ripen, metamorphism increases grain size creating a more open structure and potentially reducing capillary effects. This is indicated in the data cubes by the collection of dye along the snow layer interfaces. As snowpacks continue to ripen, dominant flow transitions from distinct meltwater flow paths to more uniform matrix flow, as illustrated by the reduced variability of many of the snow properties with respect to depth (Figures 7 and 8). This phenomenon has been observed by many others (e.g. Marsh and Woo, 1984a,b; Kattelmann and Dozier, 1999; Waldner *et al*., 2004), emphasizing that flow through a melting snowpack evolves from finger flow to matric flow that may be explained by Darcy's law as the season progresses (see review by Colbeck, 1987).

Values of wetted area for snowpacks have varied widely. Marsh and Woo (1984a) reported on ice columns formed from melt water draining into cold snowpacks and found that 22% of the area was covered with flow fingers from snowpits excavated in the Canadian Arctic near Resolute Bay and 27% of the cross-sectional area in snow from Canada's MacKenzie delta. McGurk and Kattelmann (1988) reported that about 25% of a warm snowpack was wetted by spring melt in the Sierra Nevada deep snow zone. In contrast, McGurk and Marsh (1995) from the same area report mean wetted areas of only 5, 6, and 4% from a wet and draining snowpack that had experienced considerable amounts of meltwater percolation. Our results from Experiments A and B show that a single snowpack spanned the range above, with wetted areas between stratigraphic layers ranging from 5 to 30% (Figure 7a). However, at or near stratigraphic layers the cross-sectional wetted area increased to 60%, and in one case it was as high as 95%.

Reports on the range in size and spacing of vertical flowpaths in melting snowpack also varies widely. Marsh and Woo (1984a) report flow fingers with average widths of 3·6 cm and the space between them to be 13 cm. McGurk and Kattelmann (1988) reported flow finger diameters of 5–15 cm and with the space between them of 30–50 cm. They also report that in cold, low-density snow, surface melt created smaller ice columns of less than 1 cm in diameter that were 3–10 cm apart. More recently, Campbell *et al*. (2006) used dye tracers and found that flow occurs on a wide range of scales as indicated by flow finger sizes ranging between 1 and 40 cm. In contrast, high meltwater flux at the spacing of meters has been inferred from infrared aerial photographs (Williams *et al*., 1999a) and observations of ice columns (Williams *et al*., 2000). The results from this study suggest that flowpath processes are occurring on multiple scales, even larger in extent than those suggested by Campbell *et al*. (2006). The small-scale flow indicated by the snow guillotine may fit within a larger organization of flow as indicated by Williams *et al*. (1999a, 2000). The processes underlying the spatial structure of flow cannot be identified from this study; however, our results suggest that there is multi-scale spatial organization that may provide further insight into the processes controlling flow path formation, evolution and spacing.

The snow guillotine experiments show that vertical flowpaths above and below a stratigraphic layer were not continuous. The continuity statistic for Experiment A (Figure 7d), as well as the comparison of horizontal cuts (Figure 6), illustrates continuous vertical flow within layers, with horizontal flow at layer interfaces. Using light transmission in thick horizontal sections of a melting snowpack, McGurk and Marsh (1995) also observed that meltwater flowpaths were generally continuous between thick sections within a snowpack layer, but showed little continuity across a layer interface, which they described as a melt-freeze crust. Thus, meltwater appears to aggregate at stratigraphic layers, with breakthrough below the stratigraphic horizon again causing meltwater to flow in preferential channels. However, these flow fingers were generally not contiguous with flow fingers above the stratigraphic horizon.

Layer interfaces were found to significantly affect the volume of dye, indicating dominance by lateral flow at these boundaries. These findings were supported by the decrease in probability with depth of finding vertical flow and an increase in the probability of finding lateral flow at layer interfaces. Furthermore, the connectivity statistic illustrates that there is flow coalescing at distances of 20 cm at layer interfaces, while there is little connectivity between stratigraphic layers. It is unclear whether the increase in dyed voxels at stratigraphic horizons such as buried ice layer (e.g. interface A6 in Figures 3 and 7) is because of ponding of liquid water at the layer, or movement of liquid water through the ice layer due to enhanced capillary tension within the ice layer. Williams *et al*. (2000) showed that ice columns in snowpacks can transmit high amounts of liquid water through capillary flow. The high intensity of dye in Figure 6c (at interface A6) is consistent with ponding of liquid water occurring at stratigraphic horizons.

Meltwater was found to travel laterally along at least one layer interface that was not identified upon examination of the stratigraphy within the snowpits (Figures 7 and 8). This indicates that subtle transitions in grain properties between layers may be sufficient to cause lateral flow. Other studies have reported similar findings. Waldner *et al*. (2004) used dye tracers and time domain reflectometry to observe flow responses to microstructural boundaries. They found that vertical flow at these interfaces is significantly impeded due to capillary effects. They suggested that snowpacks with larger variations in grain size, shape and density have larger capillary effects; however, Peitzsch *et al*. (2008) found that density above and below a capillary barrier was not significantly different. This study supports the finding that microstructural differences are important to the formation of capillary barriers. These barriers prevent vertical flow as characterized by large clustering of meltwater.

The fraction of the snowpack transferring liquid water was found to generally increase between experiments, but was highly variable within individual experiments with respect to depth (Figures7 and 8). Kattelmann and Dozier (1999) used a capacitance probe to measure liquid water content in a Sierra Nevada snowpack. The liquid water content was found to generally increase over time, and increased in the vicinity of layer interfaces. These findings support those of the snow guillotine experiments, in particular Experiment A. Interestingly, Kattelmann and Dozier (1999) found that liquid water content increased with depth, particularly for snowpacks above level terrain, whereas Schneebeli (1995), using fluorescent dyes, found that the fraction of snow wetted by surface melt decreased with depth in a Switzerland snowpack. This contradiction could be due to the fact that the dyed area only identifies recent water movement, while the liquid water content is a measurement of both recently generated and older liquid water.

CONCLUSION

This study presents an innovative method for measuring meltwater flow through snow using dye tracers that improves upon current field techniques. The snow guillotine allows for the unprecedented collection of high-resolution, 3D, data on meltwater flow through a snowpack at centimeter resolution. Meltwater flow was found to be strongly controlled by stratigraphic layering, with lateral flow occurring along many of the layer interfaces, even subtle ones not identified in snowpit sampling. Distinct vertical meltwater flowpaths within layers were found to be most prominent near the surface, with matric flow apparently becoming more important at depth. The occurrence of discrete meltwater flowpaths decreases the longer the snow has been isothermal. This study examines flowpaths at the centimetre-to-metre scale, proposing that flow may be correlated at very small scales that may lie within a multiple scale structure.

Furthermore, the work presented in this study emphasizes that meltwater flow is a 3D process, and capturing this nature is important for accurate 3D physically based hydrological modelling. Currently, snowmelt models do not incorporate microstructure, capillary effects, preferential flowpaths or lateral flow (Gustafsson *et al*., 2004; Waldner *et al*., 2004). The inclusion of the small-scale variability of flow illustrated by this study is important for the advancement of snowmelt hydrological modelling.

ACKNOWLEDGEMENTS

Support for this research came from a National Science Foundation grant to the Niwot Ridge Long-Term Ecological Research program (Award DEB-0423662). Logistical support was provided by the Institute of Arctic and Alpine's Mountain Research Station. Snowpit sampling was conducted in large part by undergraduate interns in Snow Hydrology (Geography 3912) under direction of the Niwot Ridge LTER field staff.

REFERENCES

Arnold N, Richards K, Willis I, Sharp M. 1998. Initial results from a distributed, physically based model of glacier hydrology. *Hydrological Processes* **12**(2).

Blöschl G, Kirnbauer R. 1991. Point snowmelt models with different degrees of complexity—Internal processes. *Journal of Hydrology* **129**(1–4): 127–147.

Caine N. 1992. Modulation of the diurnal streamflow response by the seasonal snowcover of an alpine basin. *Journal of Hydrology* **137**: 245–260.

Caine N. 1995. Snowpack influences on geomorphic processes in Green Lakes Valley, Colorado Front Range. *Geographical Journal* **161**: 55–68.

Caine N. 1996. Streamflow patterns in the alpine environment of North Boulder Creek, Colorado Front Range. *Zeitschrift fur Geomorphologie* **104**: 27–42.

Campbell F, Niewnow P, Purves R. 2006. Role of the supraglacial snowpack in mediating meltwater delivery to the glacier system as inferred from dye tracer experiments. *Hydrological Processes* **20**: 969–985. DOI: 10.1002/hyp.6115.

Colbeck SC. 1975. Theory for water-flow through a layered snowpack. *Water Resources Research* **11**(2): 261–266.

Colbeck SC. 1979. Water-flow through heterogeneous snow. *Cold Regions Science and Technology* **1**(1): 37–45.

Colbeck SC. 1987. History of snowcover research. *Journal of Glaciology* (Special Issue): 60–65.

Colbeck SC. 1991. The layered character of snow covers. *Reviews of Geophysics* **29**(1): 81–96.

Colbeck SC, Akitaya E, Armstrong R, Gubler H, Lafeuille J, Lied K, McClung D, Morris E. 1990. *The International Classification for Seasonal Snow on the Ground*. The International Commission on Snow and Ice of the International Association of Scientific Hydrology and International Glaciological Society, 22pp.

Erickson TA. 2004. *Development and application of geostatistical methods to modeling spatial variation in snowpack properties, Front Range, Colorado*. PhD dissertation, University of Colorado, Boulder, CO.

Erickson TA, Williams MW, Winstral A. 2005. Persistence of topographic controls on the spatial distribution of snow in rugged mountain terrain, Colorado, United States. *Water Resources Research* **41**(4): DOI:10.1029/2003WR002973.

Flury M, Flühler H. 1995. Tracer characteristics of Brilliant Blue FCF. *Soil Science Society of America Journal* **59**: 22–27.

Flury M, Wai NN. 2003. Dyes as tracers for vadose zone hydrology. *Reviews of Geophysics* **41**: 1–24. DOI: 10.1029/2001RG000109.

Fountain AG, Walder JS. 1998. Water flow through temperate glaciers. *Reviews of Geophysics* **36**(3): 299–328.

Gerdel RW. 1948. *Physical changes in snow-cover leading to runoff, especially to floods*. IAHS-AIHS Publication No. 31: Wallingford, UK; 42–53.

Gerdel RW. 1954. The transmission of water through snow. *Transactions of the American Geophysical Union* **35**(3): 475–485.

Gustafsson D, Waldner PA, Stähli M. 2004. Factors governing the formation and persistence of layers in a subalpine snowpack. *Hydrological Processes* **18**: 1165–1183. DOI: 10.1002/hyp.1398.

Hall DK, Riggs GA, Salomonson VV. 1995. Development of methods for mapping global snow cover using moderate resolution imaging spectroradiometer data. *Remote Sensing of Environment* **54**: 127–140.

Higuchi K, Tanaka Y. 1982. Flow pattern of meltwater in mountain snow cover. In *Hydrological Aspects of Alpine and High-Mountain Areas*. IAHS Publication No. 138. 63–69.

Kattelmann RC. 1985. Macropores in snowpacks of Sierra Nevada. *Annals of Glaciology* **6**: 272–273.

Kattelmann RC. 1989. Spatial variability of snow-pack outflow at a site in Sierra Nevada, U.S.A. *Annals of Glaciology* **13**: 124–128.

Kattelmann RC, Dozier J. 1999. Observations of snowpack ripening in the Sierra Nevada, California, U. S. A. *Journal of Glaciology* **45**(151): 409–416.

Marsh P, Woo MK. 1984a. Wetting front advance and freezing of meltwater within a snow cover, 1. Observations in the Canadian Arctic. *Water Resources Research* **20**(12): 1853–1864.

Marsh P, Woo MK. 1984b. Wetting front advance and freezing of meltwater within a snow cover, 2. a Simulation-Model. *Water Resources Research* **20**(12): 1865–1874.

Marsh P, Woo MK. 1985. Meltwater movement in natural heterogeneous snow covers. *Water Resources Research* **21**: 1710–1716.

McGurk BJ, Kattelmann RC. 1988. Transport of liquid water: flow finger evidence from thick-section photography. *Transactions of the American Geophysical Union* **69**(44): 1204.

McGurk BJ, Marsh P. 1995. Flow-finger continuity in serial thick-sections in a melting Sierran snowpack. In *Biogeochemistry of Seasonally Snow-Covered Catchments*, Tonnessen KA, Williams MW, Tranter M (eds.) *IAHS Publication* No. 228. IAHS Press: Wallingford, Oxfordshire, UK; 81–88.

Melloh RA. 1999. *A Synopsis and Comparison of Selected Snowmelt Algorithms*. U.S. Army Cold Regions Research Engineering Laboratory: Hanover, NH; 1–17.

Oda T, Kudo K. 1941. Properties of snow and its density. *Seppyo* **3**: 109–121.

Peitzsch E, Birkeland KW, Hansen KJ. 2008. Water movement and capillary barriers in a stratified and inclined snowpack. In *Proceedings of the 2008 International Snow Science Workshop*, Whistler, British Columbia. 179–187.

Racoviteanu A, Williams MW, Barry RG. 2008. Optical remote sensing of glacier characteristics: a review with focus on the Himalaya. *Sensors* **8**(5): 3355–3383. DOI: 10.3390/s8053355.

Richter-Menge JA, Colbeck SC, Jezek KC. 1991. Recent progress in snow and ice research. *Reviews of Geophysics Supplement* **29**: 218–226.

Schneebeli M. 1995. Development and stability of preferential flow paths in a layered snowpack. In *Biogeochemistry of Seasonally Snow-Covered Catchments*, Tonnessen KA, Williams MW, Tranter M (eds). *IAHS Publication* No. 228. IAHS: Wallingford, Oxfordshire, UK; 89–96.

Seligman G. 1936. *Snow Structure and Ski Fields*. J. Adams: Brussels; 555.

Stähli M, Bayard D, Wydler H, Flühler H. 2004. Snowmelt infiltration into alpine soils visualized by dye tracer technique. *Arctic Antarctic and Alpine Research* **36**(1): 128–135.

US Army. 1956. *Snow hydrology*. Summary of Report of Snow Investigations, Corps of Engineers, North Pacific Division, PB-151660, Portland, OR, 437.

Waldner PA, Schneebeli M, Schultz-Zimmermann U, Flühler H. 2004. Effect of snow structure on water flow and solute transport. *Hydrological Processes* **18**: 1271–1290. DOI: 10.1002/hyp.1401.

Wankiewicz A. 1978. Hydraulic characteristics of snow lysimeters. In *Proceedings of the Eastern Snow Conference*, 105–115.

Western AW, Blöschl G, Grayson R. 2001. Toward capturing hydrologically significant connectivity in spatial patterns. *Water Resources Research* **37**(1): 83–97.

Williams MW, Losleben M, Caine N. 1996. Changes in climate and hydrochemical responses in a high-elevation catchment in the Rocky Mountains, USA. *Limnology and Oceanography* **41**(5): 939–946.

Williams MW, Cline D, Hartmann M, Bardsley T. 1999a. Data for snowmelt model development, calibration, and verification at an alpine site, Colorado Front Range. *Water Resources Research* **35**(10): 3205–3209.

Williams MW, Sommerfield RA, Massman S, Rikkers M. 1999b. Correlation lengths of meltwater flow through ripe snowpacks, Colorado Front Range, USA. *Hydrological Processes* **13**: 1807–1826.

Williams MW, Rikkers M, Pfeffer WT. 2000. Ice columns and frozen rills in a warm snowpack, Green Lakes Valley, Colorado, U.S.A. *Nordic Hydrology* **31**(3): 169–186.

Williams MW, Seibold C, Chowanski K. 2009. Storage and release of solutes from a subalpine seasonal snowpack: Soil and stream water response, Niwot Ridge, Colorado. *Biogeochemistry* **95**(1): 77–94. DOI: 10.1007/s10533-009-9288-x.

